JOURNAL OF Applied Polymer SCIENCE

Surface Modification of Halloysite Nanotubes with L-lactic Acid: An Effective Route to High-Performance Poly(L-lactide) Composites

Wan Xu,[1] Binghong Luo,[1,2] Wei Wen,[1] Weijing Xie,[1] Xiaoying Wang,[3] Mingxian Liu,[1,2] Changren Zhou[1,2]

[1]Biomaterial Research laboratory, Department of Material Science and Engineering, College of Science and Engineering, Jinan University, Guangzhou 510632, People's Republic of China

[2]Engineering Research Center of Artificial Organs and Materials, Ministry of Education, Guangzhou 510632, People's Republic of China

[3]Department of Biomedical Engineering, College of Life Science and Technology, Jinan University, Guangzhou 510632, People's Republic of China

Correspondence to: B. luo (E-mail: tluobh@jnu.edu.cn)

ABSTRACT: To improve the interfacial bonding between halloysite nanotubes (HNTs) and poly(L-lactide) (PLLA), a simple surface modification of HNTs with L-lactic acid via direct condensation polymerization has been developed. Two modified HNTs were obtained: HNTs grafting with L-lactic acid (*l*-HNTs) and HNTs grafting with poly(L-lactide) (*p*-HNTs). The structures and properties of *l*-HNTs and *p*-HNTs were investigated. Then, a series of HNTs/PLLA, *l*-HNTs/PLLA and *p*-HNTs/PLLA composites were prepared using a solution casting method and were characterized by polarized optical microscopy (POM), field scanning electron microscopy, and tensile testing. Results showed that L-lactic acid and PLLA could be easily grafted onto the surface of HNTs by forming an Al carboxylate bond and following with condensation polymerization, and the amounts of the L-lactic acid and PLLA grafted on the surface of the HNTs were 5.08 and 14.47%, respectively. The surface-grafted L-lactic acid and PLLA played the important role in improving the interfacial bonding between the nanotubes and matrix. The *l*-HNTs and *p*-HNTs can disperse more uniformly in and show better compatibility with the PLLA matrix than untreated HNTs. As a result, the *l*-HNTs/PLLA and *p*-HNTs/PLLA composites had better tensile properties than that of the HNTs/PLLA composites. © 2014 Wiley Periodicals, Inc. J. Appl. Polym. Sci. **2015**, *132*, 41451.

KEYWORDS: clay; composites; mechanical properties; polyesters; surfaces and interfaces

Received 6 April 2014; accepted 25 August 2014
DOI: 10.1002/app.41451

INTRODUCTION

Clay–polymer composites have gained increasing interest in materials science.[1,2] Loading polymers with clay filler essentially increases the composite strength characteristics. To date, a lot of clay fillers, such as montmorillonite, kaolin, bentonite, halloysite, mogolite, and sepiolite have been introduced into the polymer matrix and many improved properties could be obtained.[3–7]

Halloysite is a naturally aluminosilicate clay with a Si/Al ratio of 1:1 and a stoichiometry of $Al_2Si_2O_5(OH)_4{\cdot}nH_2O$ (HNT). HNT is chemically similar to kaolin, but differs in possessing a regular hollow nanotubular structure with a length of 500–1000 nm and inner diameter of 15–100 nm.[8] As an easily available, inexpensive and durable material with high mechanical strength, HNT is often introduced into polymer matrix, such as polyaniline,[9] polystyrene,[10] poly(vinyl chloride),[11] rubber,[12] poly(vinyl alcohol),[13] and polyamide[14] and so forth, to prepare polymeric composites with improved mechanical performance. Furthermore, HNT nanotubes compose of siloxane groups (Si—O—Si) on the external surface and aluminol groups (Al—OH) on the internal surface, which can provide anchoring sites for surface modification with functional groups to enrich the surface chemistries of HNT.[15–18] Lvov et al. reported a selective surface modification of the inner and outer surface of HNT with octadecylphosphonic acid and organosilane coupling agents, respectively.[19] Recent studies also showed that HNT owns a biocompatible nature when HNT was used as a substrate for cell attachment and proliferation.[20] Thus, it has gained growing interest in bio-related fields, such as drug delivery system, bone implants, bioreactor and gene delivery and so forth.[21–24]

Polylactide (PLA) is an important biodegradable and biocompatible polymer with wide applications in biomedical fields, such as absorbable implants, tissue engineering scaffolds, surgical sutures, and drug-controlling release system.[25,26] However,

the mechanical strength and toughness of PLA are not strong enough for applications in biomedical materials, especially for cortical bone repair materials. To solve this problem, inorganic nanofillers, such as hydroxyapatite (HAP),[27] bio-ceramics,[28] tricalcium phosphate (TCP),[29] magnesium oxide,[30] carbon nanotubes,[31] and halloysite nanotubes (HNTs)[32,33] were introduced into PLA to enhance the mechanical properties of the material. It is well known that a better dispersion of the filler in the polymer matrix and a stronger interfacial bonding between two phases are two critical factors to improve the performance of the composites. However, it is usually difficult to obtain a good dispersion of nanofiller within a polymer matrix with high nanofiller concentration due to the tendency to aggregate. The forces in a common polymer/inorganic filler blending system include weak physical adsorption and even weaker interfacial bonding. Sliva et al. synthesized PLA/HNT films by solution casting method, and reported that a uniform dispersion of HNTs in the matrix was observed with addition less of 5 *w*/*w* % of HNTs. And yet, with the HNTs concentration increasing, an appreciable increase in the number of microvoids, pores and large particulates was observed due to the filler–matrix interaction decreasing, and the phase separation and HNT aggregation increasing.[34] Therefore, it is necessary to modify the surface of HNTs with organic groups to improve the dispersion of fillers and the interaction between two phases.

In this article, a simple and economical method was explored to modify the surface of the HNTs with L-lactic acid via direct condensation polymerization, and the effects of the surface-grafted L-lactic acid and PLLA on the properties of HNTs and HNTs/PLLA composite be studied. By this approach, not only the dispersion of the HNTs in the composite and the interfacial bonding between the HNTs and matrix would be improved, but also avoiding using the L-lactide which always needs the complicated and time-consuming preparation process.

EXPERIMENTAL

Materials

L-Lactic acid was purchased from Guangzhou Chemical Reagent Factory and purified by dehydration processing. Poly(L-lactide) (PLLA, M_w=100,000) was provided by Jinan Daigang Biology Co., HNTs, grade of ultrafine, provided by Imerys Tableware Asia Limited, New Zealand, is oven-dried at 300°C before use. Besides, calcium hydride, tetrahydrofuran, and toluene were purchased from Guangzhou Chemical Reagent Factory. All chemicals used were analytical grade.

Surface Modification of HNTs

Firstly, 5 g of HNTs were dispersed in 50 mL of tetrahydrofuran, and then a certain amount of L-lactic acid was added in dropwise under magnetic stirring. The suspension was heated to 60°C and maintained for 30 min. Then, tetrahydrofuran was removed by evaporation and 100 mL anhydrous toluene was added. After raising the temperature of the reaction system to 110°C and keeping at this temperature for 15 h, the mixture was collected via filtration and then was washed five times with tetrahydrofuran and anhydrous ethanol respectively. The residual solvent was removed under vacuum at 50°C for 24 h, and surface-modified HNTs with L-lactic acid (*l*-HNTs) were obtained.

A mixture of *l*-HNTs and L-lactic acid, and a certain amount of *p*-toluenesulfonic acid were added into a three-necked flask. The reaction mixture was heated to 150°C and maintained for 30 h, and the water formed by the polycondensation reaction was removed by azeotropic dehydration with xylene. After the reaction, the mixture was centrifuged and the precipitate was washed five times with chloroform and anhydrous ethanol respectively. After being dried in a vacuum oven at 50°C for 24 h, surface-modified HNTs with PLLA (*p*-HNTs) were obtained.

Preparation of HNTs/PLLA, *l*-HNTs/PLLA, and *p*-HNTs/PLLA Composite Membranes

HNTs/PLLA, *l*-HNTs/PLLA, and *p*-HNTs/PLLA composites with various amounts of HNTs, *l*-HNTs, and *g*-HNTs (5, 10, and 20 wt %) were prepared respectively by solution casting method using chloroform as a solvent. Briefly, the dried HNTs were suspended in chloroform to get the suspension, and 5% PLLA/chloroform solution was added into with magnetic stirring and ultrasonic treatment. Then, the mixture was poured into a Petri-dish and dried in vacuum for 24 h at 50°C, and the HNTs/PLLA composite sheets with a thickness of 0.1–0.2 mm was got. The *l*-HNTs/PLLA and *p*-HNTs/PLLA composites were prepared by the same method mentioned above.

Fourier Transformation Infrared Spectroscopy (FTIR)

All FTIR spectra were obtained using a Bruker EQUINOX55 FTIR spectrophotometer (Germany). The samples were compressed into KBr pellets for the FTIR measurements.

Thermogravimetric Analysis (TGA)

Thermogravimetric analysis was carried out with a TG 209 NETZSCH (Germany) system under nitrogen atmosphere. Samples were heated from room temperature to 600°C at a heating rate of 10°C/min.

X-ray Photoelectron Spectroscopy (XPS)

XPS spectra of the HNTs, *l*-HNTs, and *p*-HNTs were recorded using an X-ray photoelectron spectrometer (ESCALAB 250; Thermo Fisher Scientific) with an aluminum (mono) Ka source (1486.6 eV). The aluminum Ka source was operated at 15 kV and 150 W. For all the samples, a high-resolution survey (pass energy = 20 eV) was performed at spectral regions relating to silicon and aluminum atoms. The binding energy of C 1s (284.8 eV) was used as a reference.

X-ray Diffraction (XRD) Analysis

The crystal structures of the HNTs, *l*-HNTs, and *p*-HNTs were determined by a Rigaku D/max-3A diffractometer (Japan) using a Cu Kα-ray line at a scan rate of 8°/min.

Transmission Electron Microscopy (TEM) Observation

A transmission electron microscope (PHILIPS TECNAI 10) with a 200 kV acceleration voltage was used to observe the nanotubular shapes of HNTs, *l*-HNTs, and *g*-HNTs. The samples were ground into powders and dispersed in ethanol via ultrasonication. The suspension sample with a concentration of about 0.1% was obtained, and then a drop of solution was applied

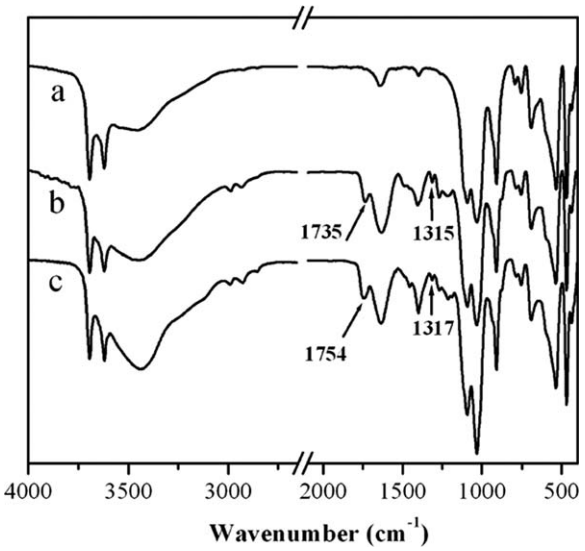

Figure 1. IR spectra of HNTs (a), *l*-HNTs (b) and *p*-HNTs (c).

onto carbon coated copper grids and left to dry in ambient condition. The final grids were used for TEM observation.

Polarized Optical Microscopy (POM) Observation

The crystal morphologies of PLLA, HNTs/PLLA, *l*-HNTs/PLLA, and *p*-HNTs/PLLA films were observed by POM (Axioskop 40; ZEISS). The films were molten at 210°C for 5 min and then cooled to 135°C at a rate of 30°C/min. The crystal morphology was observed as soon as the sample cooled to this temperature.

Field Scanning Electron Microscope (FSEM) Observation

The morphologies in the quenching fracture surfaces of the composites were observed by a FSEM (XL30 FSEM FEG; PHILIPS), a layer of gold was sprayed uniformly over the fracture surfaces before observation.

Tensile Testing

The tensile properties of PLLA, HNTs/PLLA, *l*-HNTs/PLLA, and *p*-HNTs/PLLA composite membranes were determined using a universal mechanical testing machine (AG-1 SHIMADZU). A 1 kN load-cell was used for the test. The cross-head speed was 1 mm/min. Mini dumb-bell-shaped tensile specimens with dimensions of 40 mm × 10 mm × 0.1 mm were cut from the composite membrane. Every specimen would be parallel determined five times. The averages and standard deviations were calculated.

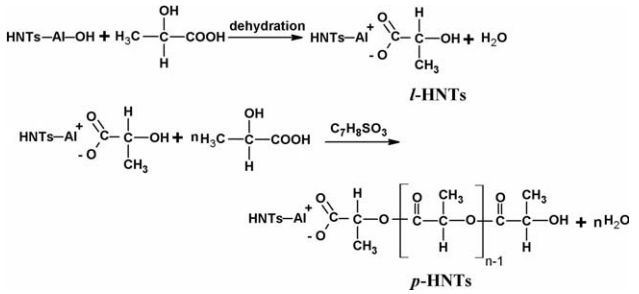

Scheme 1. Synthetic route of *l*-HNTs and *p*-HNTs.

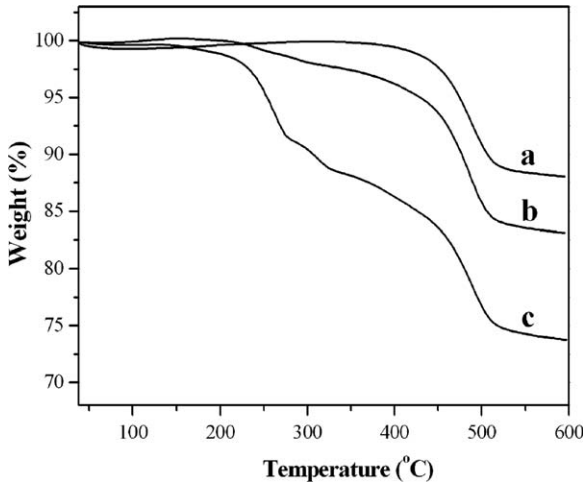

Figure 2. TG curves of HNTs (a), *l*-HNTs (b) and *p*-HNTs (c).

RESULTS AND DISCUSSION

The Structure and Properties of *l*-HNTs and *p*-HNTs

The IR spectra of HNTs, *l*-HNTs, and *p*-HNTs are shown in Figure 1. The spectrum of HNTs exhibits two Al-OH stretching vibration peaks at 3696 and 3625 cm^{-1}, and a Al-OH bending vibration peak at 619 cm^{-1}. The peak at 1034 cm^{-1} was assigned to Si—O—Si stretching vibration.[35] Compared to that of HNTs, two new absorption peaks emerged at 1315 and 1735 cm^{-1} in the spectrum of *l*-HNTs, which were attributed to the —COO— characteristic peaks of lactate. The IR spectrum of *p*-HNTs is basically the same as that of *l*-HNTs. The sample showed a characteristic peak of the lactate at 1317 cm^{-1} but did not show the peak at 1735 cm^{-1}, and a new adsorption peak at 1754 cm^{-1} attributing to the stretching vibration absorption of carbonyl group of PLLA appeared. After surface grafting with L-lactic acid and PLLA, the intensities of the characteristic vibration peaks of Al-OH decreased, but there were no significant changes in the wavenumber and intensity of the Si-O-Si absorption peak. It is likely that the grafting reaction may be mainly occurred in the AlOH groups and almost no Si—O—C bonds were formed.

It can be inferred that the surface modification reaction from the IR spectra and literature reported[36] as shown in Scheme 1. The Al—OH on the surface of HNTs can react with the carboxyl of L-lactic acid to form aluminum lactate by the condensation reaction. Then, the condensation polymerization of L-lactic acid occurred on the surface of *l*-HNTs through the lactate group using *p*-toluenesulfonic acid as a catalyst under the condition of azeotropic removal of water with xylene.

The TG curves of HNTs, *l*-HNTs, and *p*-HNTs are shown in Figure 2. It can be found that the HNTs showed a two-stage degradation pattern. The first stage in the range of 0–120°C is presumed to be the evaporation of physically absorbed water, while the second stage in the range of 400–550°C is due to the dehydroxylation of structural AlOH groups of hallyosite.[37] Compared to that of the pristine HNTs, both of the *l*-HNTs and *p*-HNTs exhibited a three-stage degradation pattern in TG thermograms. The first stage is due to the evaporation of

Table I. The Surface Element Contents of O, C, Si, and Al of HNTs, *l*-HNTs, and *p*-HNTs from XPS Analysis

	Surface element content (at %)			
Samples	O	C	Si	Al
HNTs	70.04	5.99	11.49	10.57
l-HNTs	65.32	13.99	11.01	9.18
p-HNTs	62.97	18.19	15.48	3.36

physically absorbed water, and the third one is attributed to the dehydroxylation of AlOH groups that including the inaccessible and unreacted inner surface AlOH groups of HNTs. It is obviously that the second stage in the range of 150–400°C can be ascribed to the thermal decomposition of grafted L-lactic acid and PLLA chains on the surface of *l*-HNTs and *p*-HNTs, respectively.

The amounts of the surface-grafted L-lactic acid and PLLA chains in *l*-HNTs and *p*-HNTs can be calculated as follows:

$$M(l-\text{HNTs}) = w_{\text{HNTs}} - w_{l-\text{HNTs}} = 88.18\% - 83.10\% = 5.08\%$$

$$M(p-\text{HNTs}) = w_{\text{HNTs}} - w_{p-\text{HNTs}} = 88.18\% - 73.71\% = 14.47\%$$

where w_{HNTs}, $w_{l\text{-HNTs}}$, and $w_{p\text{-HNTs}}$ are the remaining mass percentage of the HNTs, $w_{l\text{-HNTs}}$, and $w_{p\text{-HNTs}}$ at 600°C, respectively.

The XPS technique was performed to determine the changes in the surface compositions of the nanotubes before and after grafting with L-lactic acid and PLLA, and the results were given in Table I and Figure 3, respectively. It can be seen that the surface of the pristine HNTs are composed of oxygen, silicon, and aluminum, and with a Si/Al ratio of about 1.09, which is consistent with the theoretic value (1.04) calculated from the stoichiometry of $Al_2Si_2O_5(OH)_4 \cdot nH_2O$ molecules. There are a few carbon atoms on the surface of HNTs, indicating the carbon contamination may occur during sample preparation in the air.[19] After grafting with L-lactic acid and PLLA, on the one hand, the intensity of C 1s at a binding energy of 284.81 eV increased significantly, and the element contents of C of the *l*-HNTs and *p*-HNTs increased to 13.99 and 18.19%, respectively. On the other hand, the intensity of Al 2s and Al 2p at binding energy of 119.72 and 75.41 eV significantly decreased, and the element content of Al of the *l*-HNTs and *p*-HNTs decreased to 9.18 and 3.16%. The results suggested that the L-lactic acid and PLLA had been grafted onto the surface of the HNTs successfully. The intensities of binding energy of Al2s and Al2p decreased after surface grafting, it is likely to be the fact that the surfaces of the HNTs were partially wrapped with the L-lactic acid and PLLA chains, as a result, the concentration of the aluminum on the surfaces of HNTs is lower than that of the pristine HNTs.[38] Interestingly, the intensities of binding energy Si2p and Si2s of the *l*-HNTs and *p*-HNTs is just a little higher than that of the original HNTs, which indicating that the grafting reaction may be only occurred in the AlOH groups and almost no Si—O—C bonds were formed during the reaction. On the other hand, the intensity of Si2p and Si2s peaks increased slightly may be due to the silicon contamination occurred during the sample preparation.

The effects of surface-grafted L-lactic acid and PLLA oligomers on the structure of HNTs were studied by an XRD investigation, the result was shown in Figure 4. HNTs exhibited three characteristic diffraction peaks at ca. 12.49°, 20.44°, and 25.04° in 2θ, corresponding to (001), (100), and (110), respectively. After introduction of the calculated basal spacings of each plane is 0.71, 0.44, and 0.35 nm, respectively.[9] Both of the diffraction patterns of the *l*-HNTs and *p*-HNTs were basically the same as that of HNTs, which is in good agreement with our previously work reported in the literature.[33] The results indicated that the grafting reaction occurred on the internal-surface Al-OH groups of HNTs, and most of the interlayer inner-surface Al-OH groups were blocked and therefore unavailable for the grafting reaction due to the strong hydrogen bonds between interlayer. Hence, it is unlikely that the surface-grafted L-lactic acid and PLLA chains can intercalate into the interlayer of HNT to change its interlayer distances. Because of the amounts of surface-grafted L-lactic acid and PLLA chains in the *l*-HNTs and *p*-HNTs are only 5.08 and 14.47%, respectively, and too low to lead to any crystallization of the grafted chains. As a result, there is no any characteristic diffraction peak of PLLA can find in Figure 4(b,c).

Figure 5 shows the microstructures of HNTs, *l*-HNTs, and *p*-HNTs observed by TEM. The HNTs are the typical hollow

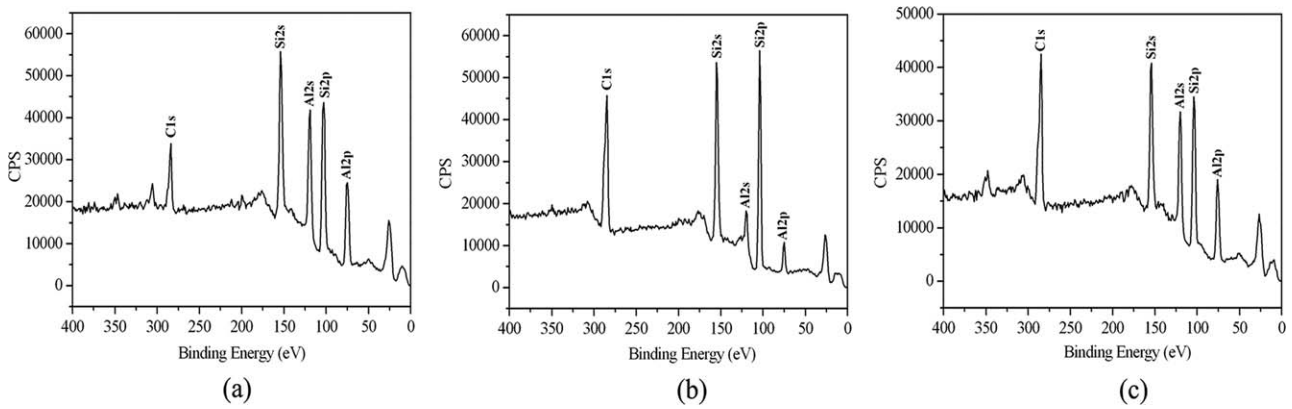

Figure 3. XPS spectra of HNTs (a), *l*-HNTs (b) and *p*-HNTs (c).

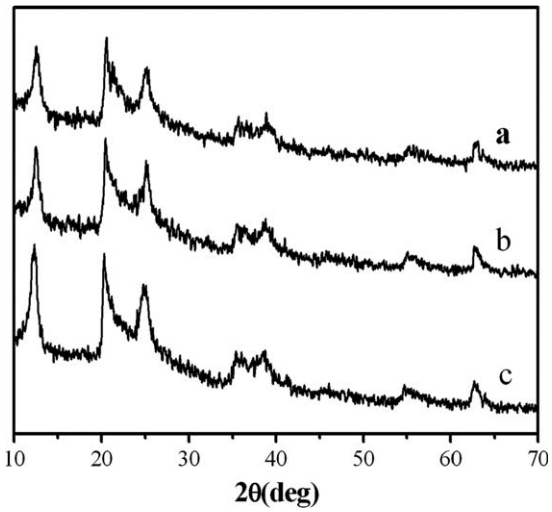

Figure 4. XRD patterns of HNTs (a), *l*-HNTs (b) and *p*-HNTs (c).

microtubes with the outer diameter of 40–70 nm and the lumen diameter of 5–15 nm. The lengths of HNTs are quite variable and in the range of 50–2000 nm. After surface-grafting with L-lactic acid and PLLA oligomer chains, there was no significant change in the shapes of *l*-HNTs and *p*-HNTs, but the dispersion of the nanotubes in ethanol was changed compared to that of HNTs. For HNTs, there is a tendency to aggregate due to the strong intermolecular hydrogen bonds of the nanotubes. After grafting with L-lactic acid on the surface of the nanotubes, the H-bonding interaction was weakened, and *l*-HNTs were uniformly dispersed in the ethanol. However, as the length of the grafted PLLA chains increasing, the *p*-HNTs tended to aggregate in the ethanol due to the hydrophobic interactions of the PLLA chains increasing.

Properties of HNT/PLlA, *l*-HNT/PLlA, and *p*-HNTs/PLlA Composite Films

In general, the crystallization rate and crystal size of polymer matrix are changed by introducing nano particles. In this article, the nucleation effect of HNTs before and after grafting with L-lactic acid and PLLA chains on the crystallization rate and morphology of PLLA matrix was observed by POM as shown in Figure 6. It can be seen that the crystallization rate of HNTs/PLLA faster than that of PLLA, and the more and smaller spherulites were formed in the HNTs/PLLA composite due to the nucleation effect of HNTs. After grafting with L-lactic acid and PLLA chains, the *l*-HNTs/PLLA, and *p*-HNTs/PLLA composite films showed much higher crystallization rate than those of the HNTs/PLLA composite and pure PLLA. These results may be due to both of the heterogeneous nucleation effects of the HNTs, grafted lactate and PLLA chains, and the excellent miscibility of the grafted HNTs with PLLA matrix.[39]

To further illustrate the effect of the incorporation of the different kinds of HNTs on the crystal properties of the PLLA matrix, XRD experiment was carried out and the result was shown in Figure 7. For pure PLLA, there are three diffraction peaks at

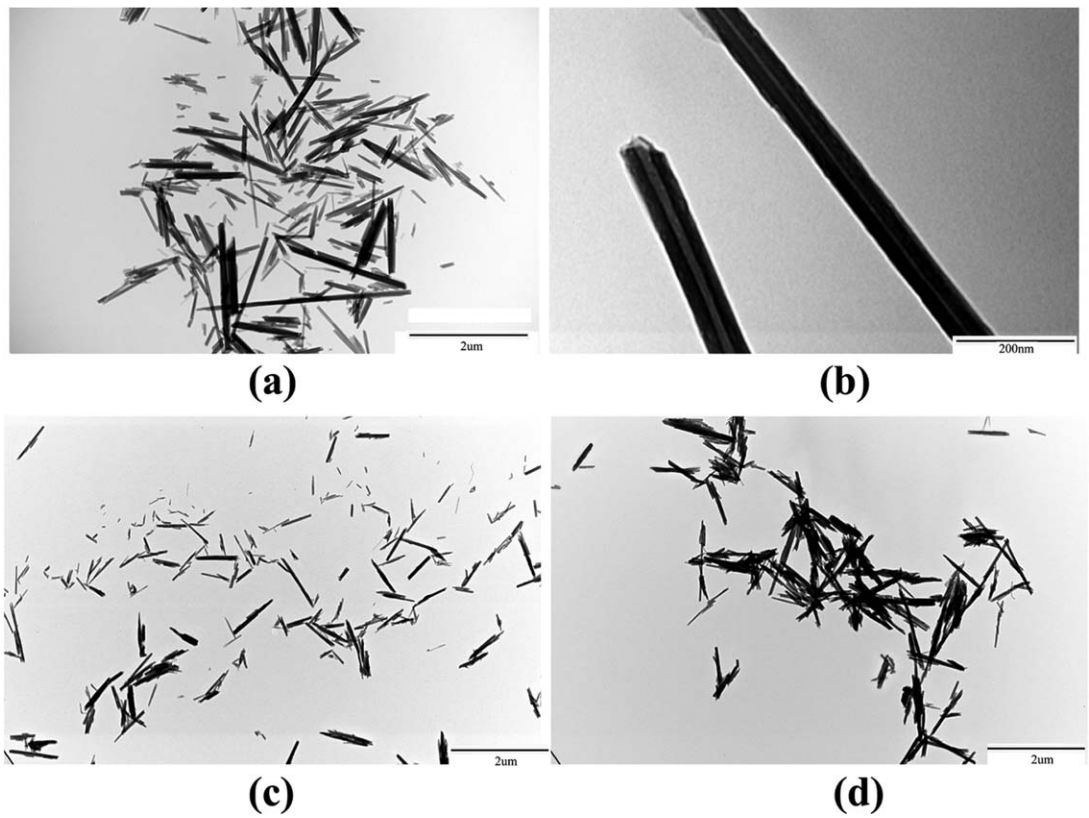

Figure 5. TEM images of the HNTs (a, b), *l*-HNTs (c) and *p*-HNTs (d) [bar = 2 um (a, c, d), bar = 200 nm (b)].

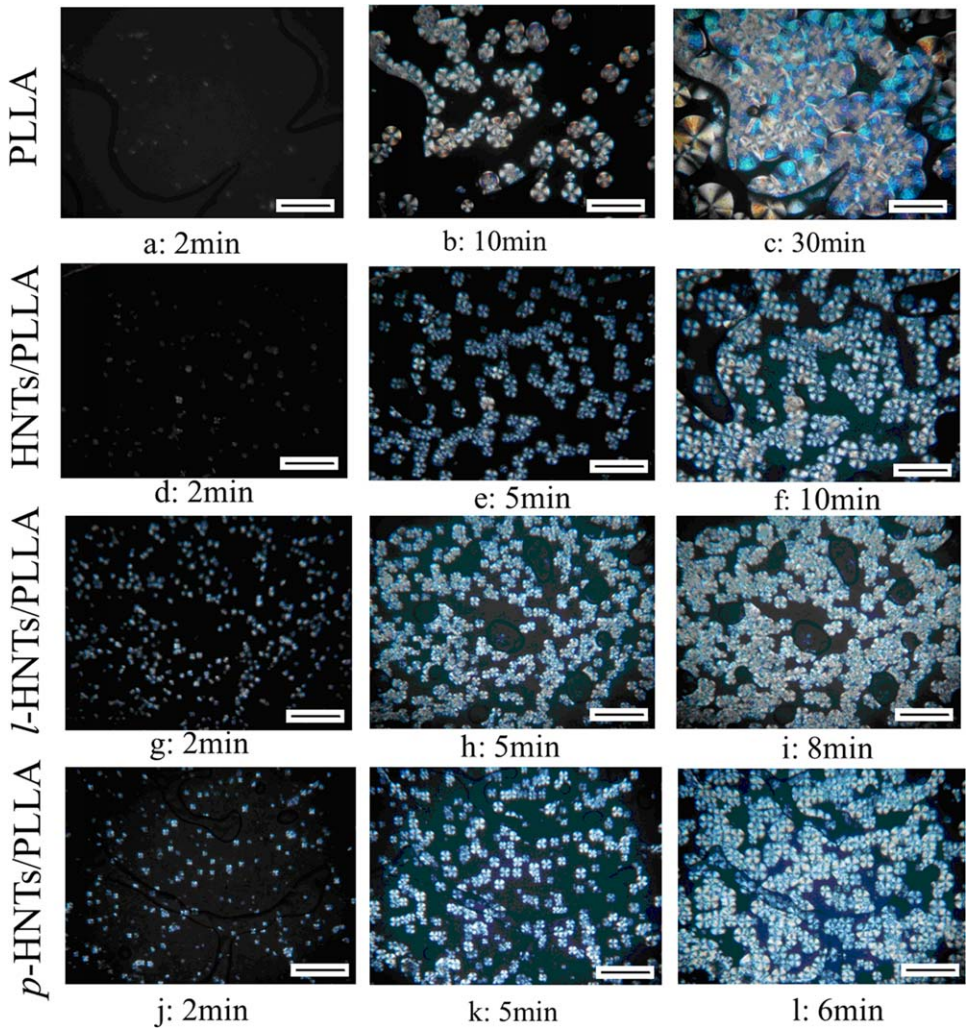

Figure 6. POM micrographs of PLLA (a, b, c), (10 wt %) HNTs/PLLA (d, e, f), (10 wt %) *l*-HNTs/PLLA (g, h, i) and (10 wt %) *p*-HNTs/PLLA (j, k, l) films (bar = 10 um). [Color figure can be viewed in the online issue, which is available at wileyonlinelibrary.com.]

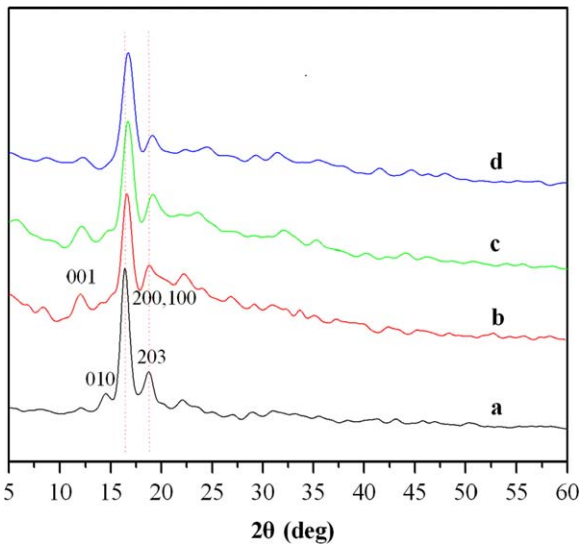

Figure 7. XRD patterns of pure PLLA (a), HNTs/PLLA (b), *l*-HNTs/PLLA(c), and *p*-HNTs/PLLA (d). [Color figure can be viewed in the online issue, which is available at wileyonlinelibrary.com.]

around $2\theta = 14.48^{o}$, 16.32^{o}, and 18.74^{o}, corresponding to the basal spacings of 0.61, 0.54, and 0.47 nm, respectively based on the Bragg equation. Introducing the HNTs, *l*-HNTs, and *p*-HNTs into the PLLA matrix, the diffraction peaks of PLLA have slightly changed and transform a little to the high 2θ. A reasonable explanation for these small changes in the diffraction peaks of PLLA matrix is that because of the heterogeneous nucleation effects of the HNTs, *l*-HNTs, and *p*-HNTs, and it is possible that the crystal structure of PLLA is transform from α' to α in the composites. The characteristic diffraction peaks of HNTs can not been observed in Figure 7(b–d) in spite of the presence of the peak at 12.16^{o} attributing to (001) due to the low content of the nanotubes in the composites.

The fracture surface morphologies of PLLA, HNTs/PLLA, *l*-HNTs/PLLA, and *p*-HNTs/PLLA composite films, and the degree of dispersion and aggregation of nanotubes in the matrix were observed by FSEM as shown in Figure 8. When the content of nanotubes was 20 wt %, most of the HNTs were seriously aggregated in the PLLA matrix, which is similar to those reported in literatures.[33,34] After surface modification of the

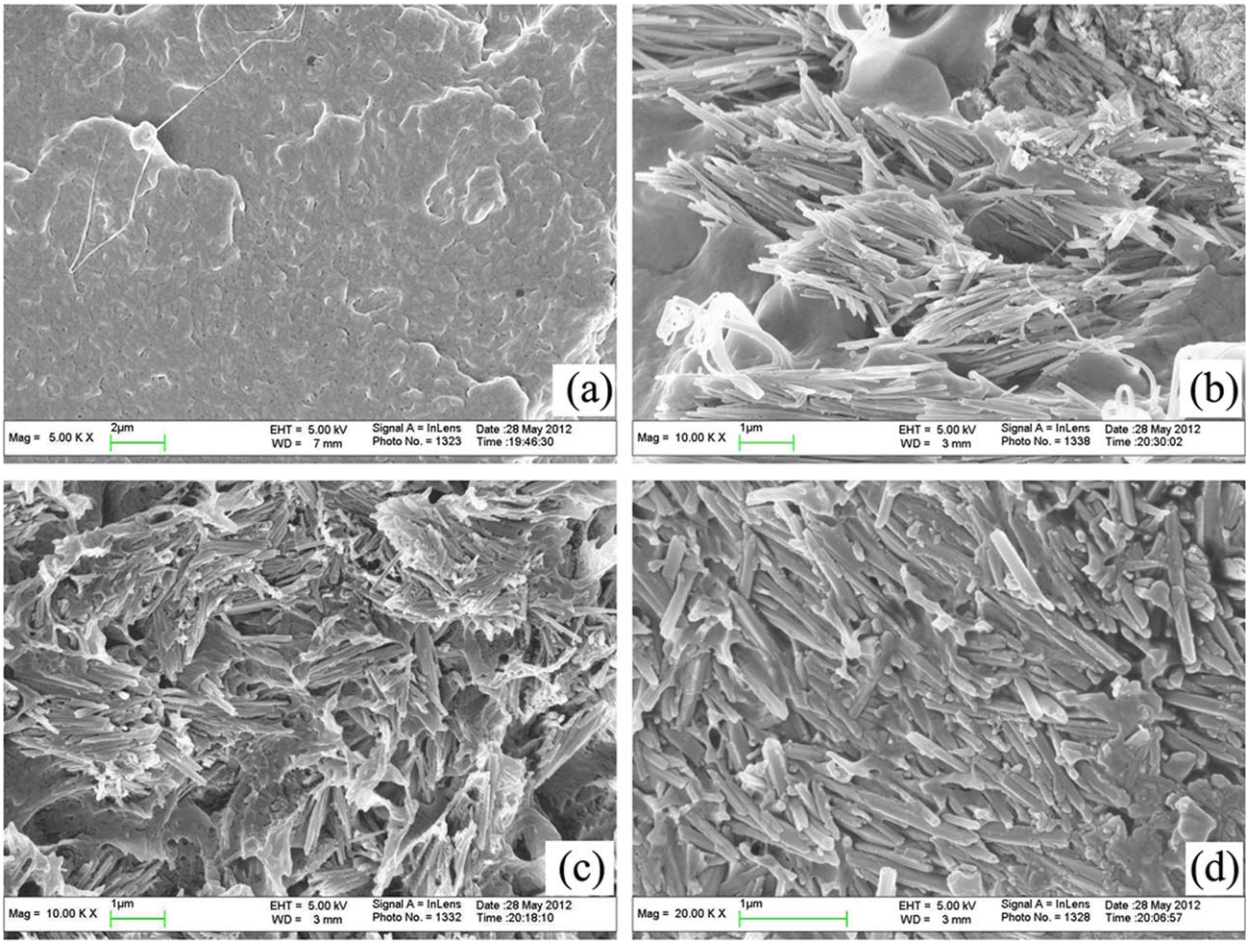

Figure 8. FSEM micrographs of fracture surfaces of PLLA (a), (20 wt %) HNTs/PLLA (b), (20 wt %) *l*-HNT/PLLA (c) and (20 wt %) *p*-HNT/PLLA (d) nanocomposite films. [Color figure can be viewed in the online issue, which is available at wileyonlinelibrary.com.]

nanotubes, the grafted L-lactic acid and PLLA chains on the surfaces of *l*-HNTs and *p*-HNTs, as inter-tying molecules, played an important role in forming the molecule chains entanglement and improving the interfacial interaction between the nanotubes and PLLA matrix phase. As a result, *l*-HNTs could be almost uniformly dispersed in PLLA matrix, and *p*-HNTs were well-dispersed in PLLA matrix as the content of the nanotubes was up to 20%.

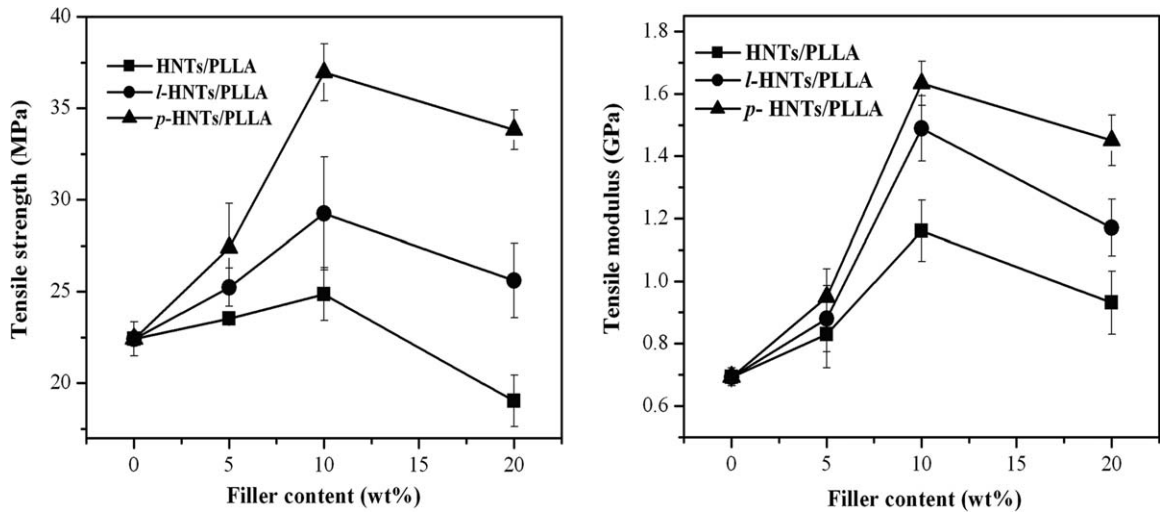

Figure 9. The dependence of tensile properties on filler content for the HNTs/PLLA (■), *l*-HNTs/PLLA (●) and *p*-HNTs/PLLA (▲) nanocomposite films.

Mechanical properties of the HNTs/PLLA, *l*-HNTs/PLLA, and *p*-HNTs/PLLA composite films were evaluated by tensile property measurement. The relationship between the tensile property and nanotube content in the composite films was demonstrated in Figure 9. With the filler content increased, the tensile strength and modulus increased firstly and then decreased, as the filler content was 10 wt %, the highest tensile strengths of 24.82, 29.74, and 37.2 MPa, and moduli of 1.15, 1.48, and 1.64 GPa were obtained for HNTs/PLLA, *l*-HNTs/PLLA, and *p*-HNTs/PLLA composite films, respectively. Obviously, not only did both the *l*-HNTs/PLLA and *p*-HNTs/PLLA composite films show higher tensile strengths and moduli than those of the HNTs/PLLA with corresponding compositions, but the *p*-HNTs/PLLA films own the highest tensile strength and modulus. It is probable that the *l*-HNTs and *p*-HNTs play an important role in improving tensile strengths and moduli of the composite films, because the grafted lactate and PLLA chains can enter the PLLA phase to entangle with and tether to the molecular chains of PLLA matrix, the longer the grafting chains, the stronger the adhesive strength between the nanotubes and PLLA matrix.

The tensile strength of HNTs/PLLA composite films is lower than that of our previous research reported for injection-moulded of PLA/HNT composites filled with 40 phr of HNTs.[40] Silva et al. reported that the maximum tensile strength of 52.75 ± 1.80 MPa and tensile modulus of 1.40 ± 0.05 GPa were achieved with addition of 5 *w*/*w* % of HNTs.[34] These differences in the results could be mainly attributed to the differences in the PLA parameters (molecular weight, crystallinity and so on), grade of HNTs and processing method. For example, the mechanical properties of solvent-casted PLLA are generally lower than that of the processed PLLA for the plasticization effects due to resudial solvent. The tensile strength of pristine PLLA used in this study is obviously lower than those of our previous study and Silva reported. By surface modification of the nanotube with PLLA chains, the tensile strength and modulus of *p*-HNTs/PLLA composite films increased by 65.7 and 142.2%, respectively with addition of 10 *w*/*w* of *p*-HNTs due to the excellent dispersion and strong interaction between two phases. This increase in tensile strength and modulus is significantly higher than that of the literatures reported.

CONCLUSIONS

In this study, two surface-modified HNTs were obtained by surface modification of HNTs with L-lactic acid via direct condensation polymerization, and the amounts of the L-lactic acid and PLLA oligomers grafted on the surface of HNTs obtained by TG was 5.08 and 14.47, respectively. The surface-grafted L-lactic acid and PLLA oligomers, as inter-tying molecules, played an important role in improving the adhesive strength between the nanotubes and PLLA matrix, which contributes to the *l*-HNTs/PLLA and *p*-HNTs/PLLA composites with the better tensile strength and modulus compared with the pristine PLLA and HNTs/PLLA.

ACKNOWLEDGMENTS

This work was supported by the national natural Science Foundation of China (No. 81171459 and 21311028), Guangdong Provincial Natural Science Foundation of China (No. 10151063201000033 and 32212055) and Scientific Cultivation and Innovation Fund of Jinan University (No. 11611439).

REFERENCES

1. Podsiadlo, P.; Kaushik, A. K.; Arruda, E. M.; Waas, A. M.; Shim, B. S.; Xu, J. D.; Nandivada, H.; Pumplin, B. G.; Lahann, J.; Ramamoorthy, A.; Kotov, N. A. *Science* **2007**, *318*, 80.
2. Bitinis, N.; Hernandez, M.; Verdejo, R.; Kenny, J. M.; Lopez-Manchado, M. A. *Adv. Mater.* **2011**, *23*, 5229.
3. Cao, H. L.; Wang, P.; Li, Y. A. *Macromol. Res.* **2010**, *18*, 1129.
4. Kongkhlang, T.; Kousaka, Y.; Umemura, T.; Nakaya, D.; Thuamthong, W.; Chirachanchai, S. *Polymer* **2008**, *49*, 1676.
5. Zhang, W.; Choi, H. *Coll. Polym. Sci.* **2012**, *290*, 1743.
6. Hapuarachchi, T. D.; Peijs, T. *Compos. Part A-Appl. S.* **2010**, *41*, 954.
7. Li, C.; Liu, J.; Qu, X.; Yang, Z. *J. Appl. Polym. Sci.* **2009**, *112*, 2647.
8. Rawtani, D.; Agrawal, Y. K. *Rev. Adv. Mater. Sci.* **2012**, *30*, 282.
9. Zhang, L.; Wang, T.; Liu, P. *Appl. Surf. Sci.* **2008**, *255*, 2091.
10. Zhao, M.; Liu, P. *J. Macromol. Sci., Part B: Phys.* **2007**, *46*, 891.
11. Liu, C.; Luo, Y.; Jia, Z.; Li, S.; Guo, B.; Jia, D. *J. Macromol. Sci. B* **2012**, *51*, 968.
12. Guo, B.; Lei, Y.; Chen, F.; Liu, X.; Du, M.; Jia, D. *Appl. Surf. Sci.* **2008**, *255*, 2715.
13. Zhou, W.; Guo, B.; Liu, M.; Liao, R.; Rabie, A. B. M.; Jia, D. *J. Biomed. Mater. Res. A* **2009**, *93*, 1574.
14. Prashantha, K.; Lacrampe, M. F.; Krawczak, P. *J. Appl. Polym. Sci.* **2013**, *130*, 313.
15. Yah, W.; Xu, H.; Soejima, H.; Ma, W.; Lvov, Y.; Takahara, A. *J. Am. Chem. Soc.* **2012**, *134*, 1853.
16. Li, C.; Liu, J.; Qu, X.; Guo, B.; Yang, Z. *J. Appl. Polym. Sci.* **2008**, *110*, 3638.
17. Joo, Y.; Jeon, Y.; Lee, S. U.; Sim, J. H.; Ryu, J.; Lee, S.; Lee, H.; Sohn, D. *J. Phys. Chem. C* **2012**, *116*, 18230.
18. Islam, M. R.; Bach, L. G.; Lim, K. T. *Appl. Surf. Sci.* **2013**, *276*, 298.
19. Yah, W. O.; Takahara, A.; Lvov, Y. M. *J. Am. Chem. Soc.* **2012**, *134*, 1853.
20. Vergaro, V.; Abdullayev, E.; Lvov, Y. M.; Zeitoun, A.; Cingolani, R.; Rinaldi, R.; Leporatti, S. *Biomacromolecules* **2010**, *11*, 820.
21. Lvov, Y. M.; Shchukin, D. G.; Mohwald, H.; Price, R. R. *ACS Nano* **2008**, *2*, 814.
22. Lvov, Y. M.; Leporatti, S. *Macromol. Biosci.* **2012**, *12*, 1265.
23. Abdullayev, E.; Lvov, Y. *J. Nanosci. Nanotechnol.* **2011**, *11*, 10007.
24. Wei, Z.; Wang, C.; Liu, H.; Zhou, S.; Tong, Z. *J. Appl. Polym. Sci.* **2012**, *125*, E358.

25. Joo-Eon, P.; Mitsugu, T. *J. Mater. Sci.-Mater. Med.* **2011**, *22*, 1171.

26. Bordes, P.; Pollet, E.; Avérous, L. *Prog. Polym. Sci.* **2009**, *34*, 125.

27. Yang, C.; Cheng, K.; Weng, W.; Yang, C. *J. Mater. Sci.-Mater. Med.* **2009**, *20*, 667.

28. Verrier, S.; Blaker, J.; Maquet, V.; Hench, L.; Boccaccini, A. R. *Biomaterials* **2004**, *25*, 3013.

29. Jung, Y.; Kim, S. S.; Kim, Y. H.; Kim, S. H.; Kim, B. S.; Kim, S.; Choi, C. Y.; Kim, S. H. *Biomaterials* **2005**, *26*, 6314.

30. Ma, F.; Lu, X.; Wang, Z.; Sun, Z.; Zhang, F.; Zheng, Y. *J. Phys. Chem. Solids.* **2011**, *72*, 111.

31. Yoon, J. T.; Lee, S. C.; Jeong, Y. G. *Comp. Sci. Technol.* **2010**, *70*, 776.

32. Wu, W.; Cao, X.; Zhang, Y.; He, G. *J. Appl. Polym. Sci.* **2013**, *130*, 443.

33. Luo, B.; Hsu, C.; Li, J.; Zhao, L.; Liu, M.; Wang, X.; Zhou, C. *J. Biomed. Nanotechnol.* **2013**, *9*, 649.

34. De Silva, R. T.; Pasbakhsh, P.; Goh, K. L.; Chai, S.-P.; Chen, J. *J. Compos. Mater. 12*, **2013**, 0021998313513046.

35. Du, M.; Guo, B.; Liu, M.; Cai, X.; Jia, D. *Physic. B-Condensed. Matter.* **2009**, *405*, 655.

36. Qiu, X.; Hong, Z.; Hu, J.; Chen, L.; Chen, X.; Jing, X. *Biomacromolecules* **2005**, *6*, 1193.

37. Yuan, P.; Southon, P. D.; Liu, Z.; Green, M. E. R.; Hook, J. M.; Antill, S. J.; Kepert, C. J. *J. Phys. Chem. C* **2008**, *112*, 15742.

38. Liu, M.; Guo, B.; Du, M.; Cai, X.; Jia, D. *Nanotechnology* **2007**, *18*, 1.

39. Hong, Z.; Zhang, P.; He, C.; Qiu, X.; Liu, A.; Chen, L.; Chen, X.; Jing, X. *Biomaterials* **2005**, *26*, 6296.

40. Liu, M.; Zhang, Y.; Zhou, C. *Appl. Clay. Sci.* **2013**, *75–76*, 52.